Intelligent Steering Control of an Autonomous Underwater Vehicle

R. Sutton, R. S. Burns

(*University of Plymouth*)

P. J. Craven

(*Racal Research Limited*)

This paper considers the development of three autopilots for controlling the yaw responses of an autonomous underwater vehicle model. The autopilot designs are based on the adaptive network-based fuzzy inference system (ANFIS), a simulated, annealing-tuned control algorithm and a traditional proportional-derivative controller. In addition, each autopilot is integrated with a line-of-sight (LOS) guidance system to test its effectiveness in steering round a series of waypoints with and without the presence of sea current disturbance. Simulation results are presented that show the overall superiority of the ANFIS approach.

KEY WORDS

1. Control. 2. Underwater Vehicles. 3. Autopilots

1. INTRODUCTION. Although remotely operated vehicles (ROVs) play an important role in the offshore industry, their operational effectiveness is limited by the tethered cable and the reliance and cost of some kind of support platform. Given these limitations and, in recent years, the concurrent developments in advanced control engineering theory, artificial intelligence (AI) techniques and computation hardware for analysis, design and implementation, interest in the viability of employing autonomous underwater vehicles (AUVs) in operational tasks has been rekindled. Indeed, the potential usage of AUVs was recognised in the recently published report by the Marine Foresight Panel.[1] The report considered that AUVs will be able to provide essential platforms for instruments and sensors for various kinds of subsea missions in the near future. These missions could include: environmental forecasting, policing exclusive economic zones and under-ice operations as well as ocean basin monitoring in the Global Ocean Observing System.[2] AUVs equipped with side-scan sonar may also take part in topographic mapping surveys or undertake pipeline inspections. In addition, from a naval viewpoint, suitably fitted vehicles could be deployed for mine countermeasures, mine laying and covert surveillance sorties. For the interested reader a comprehensive list of AUVs existing worldwide can be found in Reference 3 and on http://www.acim.usl.edu/~maja/AUV/AUV-list.html.

From the aforementioned, the impression may have been given that AUVs are going to become the imminent panacea for a number of subsea activities. This is certainly not the case for AUVs intended for long duration missions because of three main reasons. The first is a non-technical matter that needs to be resolved as soon as

possible and revolves around the legal responsibilities and liabilities for AUVs deployed at sea. Without doubt, these are issues that need to be clarified; however, they are clearly outside the scope of this paper. The second reason relates to the limited endurance capacity of the power systems. Most AUVs depend on battery power which, inevitably, limits their range. To overcome this problem, there needs to be a major breakthrough in battery technology or a shift to other power sources such as non air-breathing diesel plant. The third and final restricting factor is associated with the capabilities of the current generation of onboard navigation, guidance and control (NGC) systems.

For this type of vehicle to be truly autonomous, it needs to possess a reliable and robust NGC system, of which a key element is the control subsystem responsible for maintaining the vehicle on course. Several advanced control engineering concepts including: $H\infty$,[4] sliding mode,[5] and predictive control[6] are being employed in the design of course-changing autopilots and have met with varying degrees of success. AI approaches are also being introduced into the design process. Autopilots formulated using fuzzy logic and artificial neural network (ANN) methods have been reported and shown to be commendably robust. Encouraged by such results, this paper considers the development of a course-changing autopilot based on the innovative neuro-fuzzy methodology of Jang[7] known as the adaptive network-based fuzzy inference system (ANFIS) that was successfully employed to produce a control strategy for the classical inverted pendulum problem.

With the ANFIS approach, implementation of the controller design differs in form from the more usual ANN in that it is not fully connected, and not all the weights or nodal parameters are modifiable. Essentially the fuzzy rule base is encoded in a parallel fashion so that all the rules are activated simultaneously to allow network training algorithms to be applied. As in Jang's original work, a back-propagation algorithm is used to optimise the fuzzy sets of the antecedents in the ANFIS architecture, and a least squares procedure is applied to the linear coefficients in the consequent terms.

For performance assessment purposes, the ANFIS design is compared to that of a simulated annealing (SA)-tuned autopilot and a proportional-derivative controller. In the design of the SA-tuned autopilot, an adaptive structure similar to the ANFIS architecture is employed. However, during its tuning process, the input data are only fed forward through the network in order to generate an error function. The SA algorithm is then applied to optimise the premise parameters.

The paper also considers the performance of a guidance subsystem based on a line-of-sight (LOS) algorithm. Throughout this simulation study, the test bed platform for evaluating the control algorithms is a generic AUV dynamic model that is currently being employed by the Defence Evaluation and Research Agency (DERA), Sea Systems Sector, Winfrith, in a number of their integrated control systems design studies.

2. MODELLING THE AUTONOMOUS UNDERWATER VEHICLE DYNAMICS.

Figure 1 shows the complete control authority of the AUV model. However, it should be noted that for this study the upper and lower canards are the only surfaces used to control its yaw dynamics. Dimensionally, the model represents an underwater vehicle that is 7 metres long, 1 metre in diameter and has a displacement of 3600 kilogrammes.

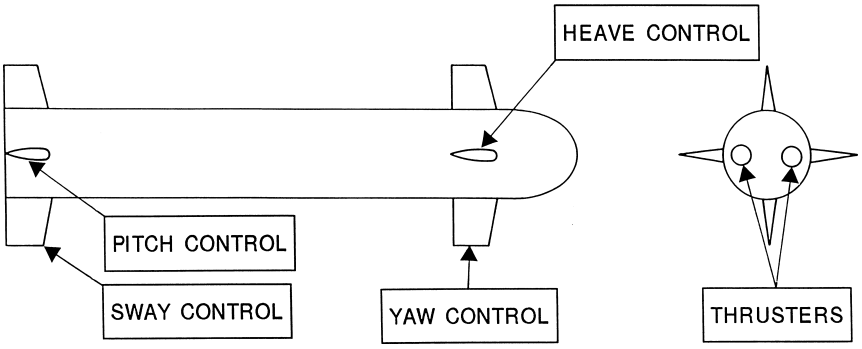

Figure 1. Complete control authority of the AUV model.

A full description of the equations of motion describing the dynamic behaviour of the vehicle in the lateral plane can be found in Reference 8. Throughout this study, use is made of an AUV MATLAB/Simulink simulation model supplied by DERA, Winfrith. The model having been validated against standard DERA non-linear hydrodynamic code using tank test data and an experimentally derived set of hydrodynamic coefficients from the Southampton Oceanography Centre's AUTOSUB vehicle. In addition, the MATLAB/Simulink model structure also takes into account the dynamic behaviour of the canard actuators by describing them as first order lags with appropriate limiters.

3. NEURO-FUZZY AUTOPILOT DESIGN. As discussed above, the fuzzy controller design used in this study is based on the ANFIS. Functionally, there are almost no constraints on the membership functions of an adaptive network except piecewise differentiability. Structurally, the only limitation on network configuration is that it should be of the feed-forward type. Due to these minimal restrictions, the adaptive network's applications are immediate and immense in various areas. If it is assumed that the fuzzy inference system under consideration has multiple inputs and one functional output (f), then the fuzzy rule-based algorithm may be represented in the first order Sugeno form as shown below:

Rule 1: If x is A_1 and y is B_1 then $f_1 = p_1\ x + q_1\ y + r_1$

Rule 2: If x is A_2 and y is B_2 then $f_2 = p_2\ x + q_2\ y + r_2$

: : : : : : :

: : : : : : :

Rule n: If x is A_n and y is B_n then $f_n = p_n\ x + q_n\ y + r_n$

The corresponding ANFIS architecture is shown in Figure 2.

The node functions in the same layer are of the same function family as described by the following:

Layer 1 – Every ith node in this layer is an adaptive node with a node output defined by:

$$O_{1,i} = \mu_{A_i}(x) \tag{1}$$

where: x is the input to the general node, and A_i is the fuzzy set associated with this node. In other words, outputs of this layer are the membership values of the premise part. Here the membership functions for A_i can be any appropriate

https://doi.org/10.1017/S0373463300008973 Published online by Cambridge University Press

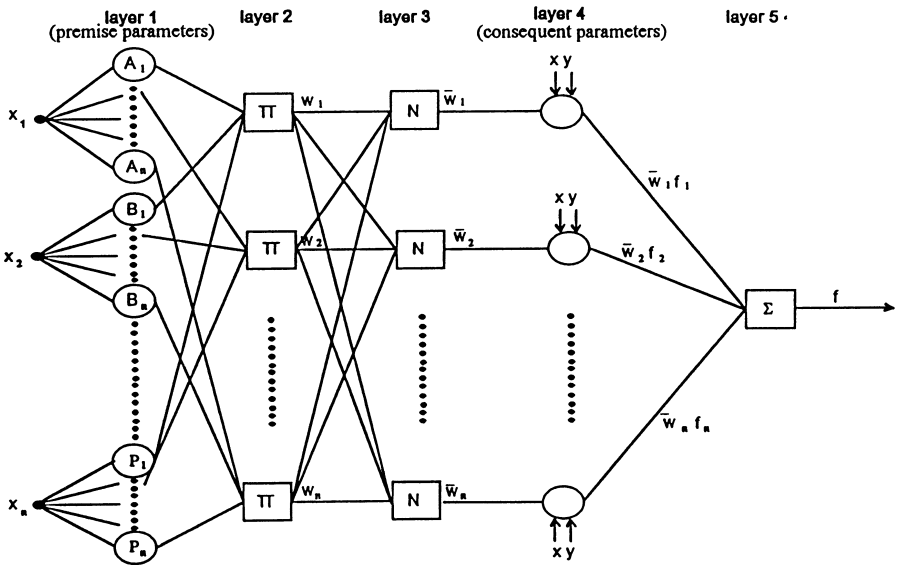

Figure 2. The adaptive network-based fuzzy inference system architecture.

parameterised membership functions. Here A_i is characterised by the generalised bell function:

$$\mu_{A_i}(x) = \frac{1}{1+\left[\left(\frac{x-c_i}{a_i}\right)^2\right]^{b_i}} \tag{2}$$

where: $\{a_i, b_i, c_i\}$ is the parameter set. Parameters in this layer are referred to as *premise parameters*.

Layer 2 – Every node in this layer is a fixed node labelled Π, which multiplies the incoming signals and outputs the product or T-norm operator result, for example:

$$O_{2,i} = w_i = \mu_{A_i}(x) \times \mu_{B_i}(y), \quad i = 1, 2. \tag{3}$$

Each node output represents the *firing strength* of a rule. (In fact, any other T-norm operators that perform the fuzzy AND operation can be used as the node function in this layer.)

Layer 3 – Every node in this layer is a fixed node labelled N. The *i*th node calculates the ratio of the *i*th rule's firing strength to the sum of all rules' firing strengths:

$$O_{3,i} = \bar{w}_i = \frac{w_i}{w_1 + w_2}, \quad i = 1, 2. \tag{4}$$

For convenience, outputs of this layer are called *normalised firing strengths*.

Layer 4 – Every *i*th node in this layer is an adaptive node with a node function:

$$O_{4,i} = \bar{w}_i f_i = \bar{w}_i(p_i x + q_i y + r_i) \tag{5}$$

where $\bar{w}_i$ is the output of Layer 3 and $\{p_i, q_i, r_i\}$ is the parameter set. Parameters in this layer are referred to as *consequent parameters*.

https://doi.org/10.1017/S0373463300008973 Published online by Cambridge University Press

Layer 5 – The single node in this layer is labelled Σ, which computes the overall output as the summation of incoming signals:

$$O_{5,i} = \text{overall output} = \sum_i \bar{w}_i f_i = \frac{\sum_i w_i f_i}{\sum_i w_i} \tag{6}$$

Thus an adaptive network that has exactly the same function as a Sugeno fuzzy model may be constructed.

4. SIMULATED ANNEALING TUNED AUTOPILOT STRUCTURE.

The structure of the SA-tuned autopilot is similar to that described in section 3 and depicted in Figure 3. However, there are dissimilarities. In this case, the nodes in Layer 4 are static and therefore are not modifiable. Also during the tuning process, input data are only fed forward through the network in order to generate an error function. The SA algorithm is then applied to optimise the premises.

5. THE TRAINING ALGORITHMS.

5.1. *The Hybrid Learning Rules.* Rewriting the premise membership function Equation 2 as:

$$\mu_{ij}(x) = \frac{1}{1+\left[\left(\frac{x-c_{ij}}{a_{ij}}\right)^2\right]^{b_{ij}}} \tag{7}$$

Equation 7 now represents the jth membership function on the ith input universe of discourse. Therefore the learning rule for a general parameter may be described as follows:

$$\begin{aligned}\Delta\alpha_{ij} &= -\eta \cdot \sum_{n=1}^{P} \frac{\partial E_n}{\partial O^i_{1n}} \cdot \frac{\partial O^i_{1n}}{\partial \alpha_{ij}} \\ &= -\eta \cdot \sum_{n=1}^{P} \frac{\partial E_n}{\partial O^{ij}_{2n}} \cdot \frac{\partial O^{ij}_{2n}}{\partial O^{ij}_{1n}} \cdot \frac{\partial O^{ij}_{1n}}{\partial \alpha_{ij}}\end{aligned} \tag{8}$$

Hence, as shown in Reference 8, the learning rules for each individual parameter are:

$$\Delta a_{ij} = -\eta \cdot \sum_{n=1}^{P} \frac{\partial E_n}{\partial O^{ij}_{2n}} \cdot \frac{\partial O^{ij}_{2n}}{\partial O^{ij}_{1n}} \cdot \left[\frac{2b_{ij}a_{ij}^{(2b_{ij}-1)}(x-c_{ij})a_{ij}^{2b_{ij}}(x-c_{ij})^{2b_{ij}}}{\{a_{ij}^{2b_{ij}}(x-c_{ij})^{2b_{ij}}+(x-c_{ij})^{2b_{ij}}a_{ij}^{2b_{ij}}\}^2}\right] \tag{9}$$

$$\Delta b_{ij} = -\eta \cdot \sum_{n=1}^{P} \frac{\partial E_n}{\partial O^{ij}_{2n}} \cdot \frac{\partial O^{ij}_{2n}}{\partial O^{ij}_{1n}} \cdot \left[\frac{2a_{ij}^{2b_{ij}}(x-c_{ij})^{2b_{ij}}\, a_{ij}^{2b_{ij}}(x-c_{ij})^{2b_{ij}} \ln\left[\left|\frac{a_{ij}}{x-c_{ij}}\right|\right]}{\{a_{ij}^{2b_{ij}}(x-c_{ij})^{2b_{ij}}+(x-c_{ij})^{2b_{ij}}a_{ij}^{2b_{ij}}\}^2}\right] \tag{10}$$

$$\Delta c_{ij} = -\eta \cdot \sum_{n=1}^{P} \frac{\partial E_n}{\partial O^{ij}_{2n}} \cdot \frac{\partial O^{ij}_{2n}}{\partial O^{ij}_{1n}} \cdot \left[\frac{-2b_{ij}a_{ij}^{2b_{ij}}(c_{ij}-x)a^{(2b_{ij}-1)}\, a_{ij}^{2b_{ij}}(-(x-c_{ij}))^{2b_{ij}}}{\{a_{ij}^{2b_{ij}}(-(x-c_{ij})^{2b_{ij}}+(c_{ij}-x)^{2b_{ij}}a_{ij}^{2b_{ij}}\}^2}\right] \tag{11}$$

The fuzzy consequent parameters being updated using a recursive least squares method as also described in Reference 8.

5.2. *Simulated Annealing.* The main problem associated with gradient descent-based learning algorithms for optimisation problems, such as backpropagation, is the tendency for these methods to spend long periods of time in the neighbourhood of poor or sub-optimal local minima on the error hypersurface. A technique that can be employed to overcome this shortcoming is SA, which was first introduced at

https://doi.org/10.1017/S0373463300008973 Published online by Cambridge University Press

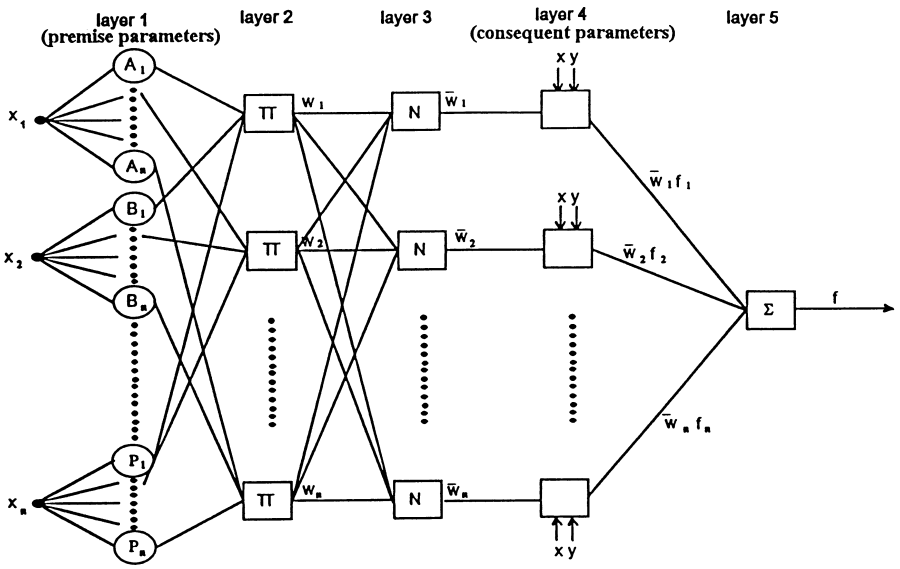

Figure 3. The structure of the simulated annealing tuned autopilot.

Reference 9. SA is a very efficient random search method for global minimisation. This method is based on an analogy between the global minimisation problem and that of determining the lowest energy state of a physical system. Kirkpatrick *et al.*[9] adapted an algorithm taken from the statistical mechanics field for converging to one of many possible cooled or low energy states. Energies of this algorithm are described by a Boltzman probability distribution such that the probability of any given energy E is an exponentially decreasing function of E. Thus, if a new matrix of parameters θ, which have been perturbed from an initially assumed solution by a randomly generated amount, lead to an improved performance of the system under consideration, then they are accepted and the process is repeated. However, if this new matrix leads to a worsened performance of the system it may be occasionally accepted with probability $P(\theta)$ such that:

$$P(\theta) = \exp\left[\frac{-E(\theta)}{kT}\right], \tag{12}$$

where: $E(\theta)$ is the energy associated with the state θ, k is the Boltzman's constant and T is a temperature parameter.

For a thermodynamic system, it can be demonstrated both by theoretical arguments and experimental verification that the most effective strategy for obtaining a global minimum energy state requires the temperature to be cooled slowly. Indeed, provided the cooling process is performed sufficiently slowly, the system will by-pass locally stable states to reach one that is a global minimum. Thus, in analogous systems, the temperature T is allowed to decay during training according to the following equation:

$$T = \frac{T_o}{1 + an} \tag{13}$$

https://doi.org/10.1017/S0373463300008973 Published online by Cambridge University Press

where: T_o is the initial temperature, a is a constant which governs the decay rate and n is the training epoch. Hence, SA may be considered to consist of three distinct phases:

i a random search step;
ii a minimisation stage, and
iii a stopping rule.

The random search step is basically the iterative generation of random matrices in a domain $S(\theta_k)$. The minimisation stage consists of applying a local minimisation routine to some of the sampled matrices, whilst the stopping rule terminates the algorithm provided there is sufficient evidence that the global minimum has been detected within the limits of a specified accuracy or some explicit iteration number is reached. In summary, the SA algorithm can be expressed as in Table 1.

Table 1. Simulated annealing algorithm.

1.	Generate set of initial parameters and simulate system.
2.	Make random changes to the parameters and re-simulate the system.
3.	If performance improved then retain changes and re-apply.
4.	If performance degraded then compute probability of accepting poorer parameters according to equations (12) and (13).
5.	Generate random number in the range 0–1 and compare with probability computed at 4. If random number less then accept poorer parameters; otherwise reject.
6.	Re-simulate and return to 3 until convergence.

6. PROPORTIONAL-DERIVATIVE AUTOPILOT DESIGN. Whilst a number of advanced approaches are now being applied to the control of AUVs, there are still a number of craft employing autopilot designs based on variants of the classical proportional-integrate derivative (PID) controller. Such a controller can be represented by a non-interacting structure in the Laplace domain as:

$$\frac{u}{e}(s) = K\left[1 + \frac{1}{T_I s} + T_d s\right]. \tag{14}$$

For this study, it was expedient to use a PD controller as a benchmark and, therefore, Equation 14 is reduced to:

$$\frac{u}{e}(s) = K[1 + T_d s]. \tag{15}$$

The parameters K and T_d were obtained using a Ziegler and Nichols method. From a practical viewpoint, it is customary to limit the bandwidth of the derivative action to approximately half a decade. By restricting the derivative bandwidth, the benefits of derivative action are maintained without too much amplification of high frequency noise. Thus, the PD autopilot design is taken as:

$$\frac{u}{e}(s) = \frac{0{\cdot}007[1 + 0{\cdot}643\, s]}{[1 + 0{\cdot}117\, s]} \tag{16}$$

https://doi.org/10.1017/S0373463300008973 Published online by Cambridge University Press

7. WAYPOINT GUIDANCE BY LINE-OF-SIGHT (LOS). LOS guidance algorithms are more usually associated with airborne missile systems. Nevertheless, based on the work of Healey and Lienard,[10] guidance of the AUV model is realised here by a heading command to the steering mechanism of the vehicle to approach the LOS between its present position and the next waypoint. Ideally, the design of the guidance and control systems should be fully integrated. Although this is not the case in this study, it is assumed the autopilot has a sufficiently large bandwidth to track the commands from the guidance subsystem. As consideration is only being given to the vehicle operating in the lateral plane, then the LOS is defined as the horizontal angle given by:

$$\psi_d = \tan^{-1}\left[\frac{(y_k - y(t))}{(x_k - x(t))}\right] \tag{17}$$

where: $\{x_k, y_k\}$ are the waypoints stored in the mission planner of the AUV and $\{x(t), y(t)\}$ are the current co-ordinates as shown in Figure 4. It is pointed out in Reference

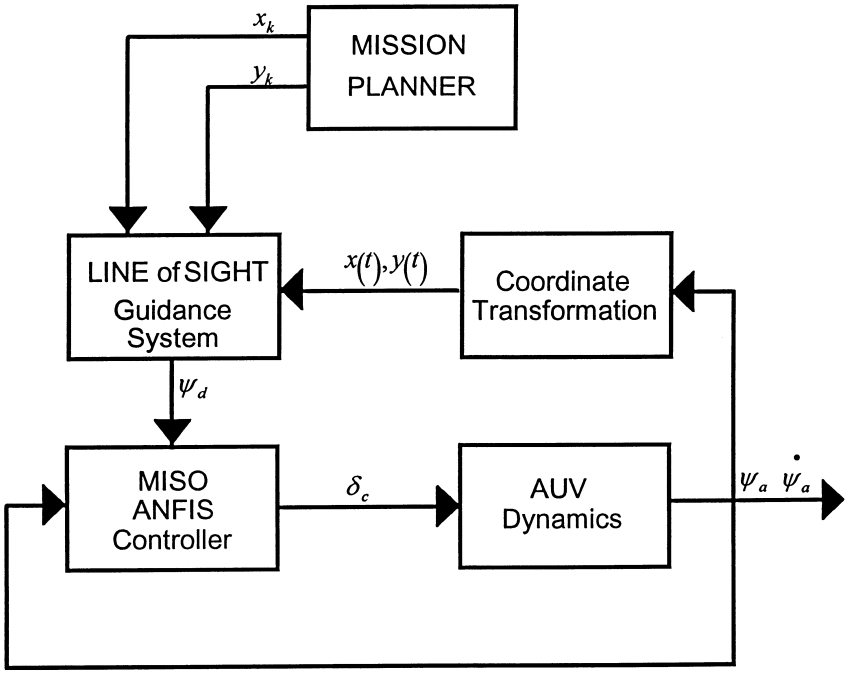

Figure 4. Line-of-sight guidance system for the AUV.

10 that care must be exercised to ensure the proper quadrant is selected when programming the guidance law. In order to inform the AUV that it has reached a given waypoint, a 'circle of acceptance' having a radius ρ_{CA} is defined:

$$\rho^2(t) = [x_k - x(t)]^2 + [y_k - y(t)]^2 < {\rho_{CA}}^2 \tag{18}$$

For this study, the radius was taken as being three times the length of the AUV.

https://doi.org/10.1017/S0373463300008973 Published online by Cambridge University Press

8. RESULTS AND DISCUSSION. Tuning algorithms based upon the ANFIS and SA techniques have been developed and applied to the task of tuning course-changing fuzzy autopilots for an AUV. This section discusses the performance of each autopilot in a qualitative and quantitative manner and makes comparisons to a traditional PD autopilot. For completeness, results are presented that detail autopilot robustness to parameter variations and sea current disturbances, and to the more general capability to accept course-changing demands that were not used as training data in the tuning process.

Tuning of the fuzzy autopilot parameters took place over a series of positive and negative course-changing demands of 40° at a surge velocity of 7·5 knots. Sufficient time intervals were given between consecutive course-changing demands to enable the AUV translational and rotational motions to stabilise, and thus ensure that each course-change was applied at similar initial conditions. This method was employed to affect symmetry within the final membership functions and rules of the neurally-tuned fuzzy autopilots.

The ANFIS technique was applied to the task of tuning both the premise and consequent parameters of a nine-rule fuzzy autopilot of Sugeno form, using the hybrid learning rule outlined in section 5.1. The resulting linear fuzzy rules are of the form:

$$
\begin{aligned}
&\text{If } \psi_\epsilon \text{ is } N \text{ and } \dot{\psi} \text{ is } N \text{ then } \delta = -1{\cdot}46\,\psi_\epsilon - 0{\cdot}89\,\dot{\psi} + 0{\cdot}66\\
&\text{If } \psi_\epsilon \text{ is } N \text{ and } \dot{\psi} \text{ is } Z \text{ then } \delta = -0{\cdot}49\,\psi_\epsilon - 0{\cdot}88\,\dot{\psi} - 0{\cdot}05\\
&\text{If } \psi_\epsilon \text{ is } N \text{ and } \dot{\psi} \text{ is } P \text{ then } \delta = -0{\cdot}51\,\psi_\epsilon - 0{\cdot}89\,\dot{\psi} - 0{\cdot}69\\
&\text{If } \psi_\epsilon \text{ is } Z \text{ and } \dot{\psi} \text{ is } N \text{ then } \delta = -0{\cdot}45\,\psi_\epsilon - 0{\cdot}11\,\dot{\psi} + 0{\cdot}79\\
&\text{If } \psi_\epsilon \text{ is } Z \text{ and } \dot{\psi} \text{ is } Z \text{ then } \delta = -0{\cdot}00\,\psi_\epsilon - 0{\cdot}00\,\dot{\psi} + 0{\cdot}00\\
&\text{If } \psi_\epsilon \text{ is } Z \text{ and } \dot{\psi} \text{ is } P \text{ then } \delta = -0{\cdot}45\,\psi_\epsilon - 0{\cdot}11\,\dot{\psi} - 0{\cdot}79\\
&\text{If } \psi_\epsilon \text{ is } P \text{ and } \dot{\psi} \text{ is } N \text{ then } \delta = -0{\cdot}51\,\psi_\epsilon - 0{\cdot}89\,\dot{\psi} + 0{\cdot}69\\
&\text{If } \psi_\epsilon \text{ is } P \text{ and } \dot{\psi} \text{ is } Z \text{ then } \delta = -0{\cdot}49\,\psi_\epsilon - 0{\cdot}88\,\dot{\psi} + 0{\cdot}05\\
&\text{If } \psi_\epsilon \text{ is } P \text{ and } \dot{\psi} \text{ is } P \text{ then } \delta = -1{\cdot}46\,\psi_\epsilon - 0{\cdot}89\,\dot{\psi} - 0{\cdot}66
\end{aligned}
\tag{19}
$$

In addition, the SA algorithm outlined in section 5.2 was applied to the task of tuning only the premise parameters of the same nine-rule Sugeno fuzzy autopilot, whilst the consequent parameters remained fixed as equally spaced singletons upon the output universe of discourse.

The tuning regime resulted in the following fuzzy rule base:

$$
\begin{aligned}
&\text{If } \psi_\epsilon \text{ is } N \text{ and } \dot{\psi} \text{ is } N \text{ then } \delta = +25{\cdot}00\\
&\text{If } \psi_\epsilon \text{ is } N \text{ and } \dot{\psi} \text{ is } Z \text{ then } \delta = +18{\cdot}75\\
&\text{If } \psi_\epsilon \text{ is } N \text{ and } \dot{\psi} \text{ is } P \text{ then } \delta = +12{\cdot}50\\
&\text{If } \psi_\epsilon \text{ is } Z \text{ and } \dot{\psi} \text{ is } N \text{ then } \delta = +6{\cdot}25\\
&\text{If } \psi_\epsilon \text{ is } Z \text{ and } \dot{\psi} \text{ is } Z \text{ then } \delta = 0{\cdot}00\\
&\text{If } \psi_\epsilon \text{ is } Z \text{ and } \dot{\psi} \text{ is } P \text{ then } \delta = -6{\cdot}25\\
&\text{If } \psi_\epsilon \text{ is } P \text{ and } \dot{\psi} \text{ is } N \text{ then } \delta = -12{\cdot}50\\
&\text{If } \psi_\epsilon \text{ is } P \text{ and } \dot{\psi} \text{ is } Z \text{ then } \delta = -18{\cdot}75\\
&\text{If } \psi_\epsilon \text{ is } P \text{ and } \dot{\psi} \text{ is } P \text{ then } \delta = -25{\cdot}00
\end{aligned}
\tag{20}
$$

https://doi.org/10.1017/S0373463300008973 Published online by Cambridge University Press

A qualitative assessment of autopilot responsiveness was provided by the AUV model's responses to a series of positive and negative course-changing demands of varying magnitude, as illustrated in Figure 5. Such a track configuration was deemed

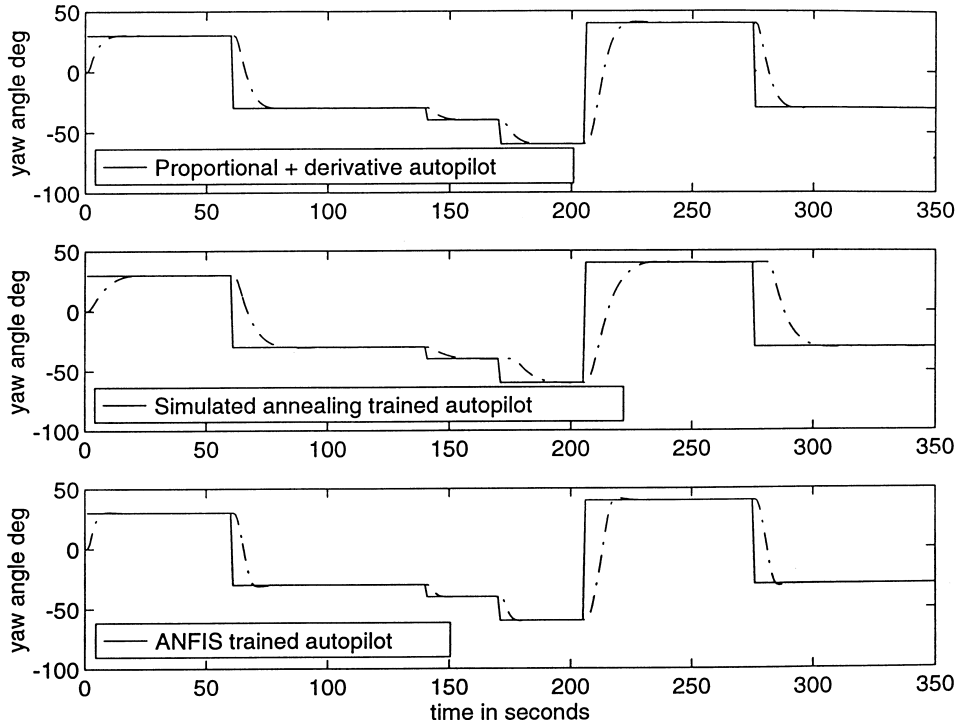

Figure 5. Yaw responses of the AUV over the validation track.

necessary to assess the ability of each autopilot to generalise to course-changes for which they had not been tuned. Figure 6 shows the corresponding canard demands to the track configuration of Figure 5.

The ANFIS-tuned fuzzy autopilot displayed the most accurate response over this particular track configuration, with smaller rise times and no steady-state course error. Collectively these responses suggest that the hybrid learning rule employed by the ANFIS tuning regime was the most effective at producing a tuned autopilot with reduced off-course error with good generalisation qualities. As a means of quantifying off-course error and course-changing control effort the following performance measures were adopted:

$$\psi_\epsilon = \int_{t_1}^{t_2} (\psi_d - \psi_a)^2 \, \mathrm{d}t, \tag{21}$$

$$\psi_\epsilon = \int_{t_1}^{t_2} (\delta_d - \delta_a)^2 \, \mathrm{d}t, \tag{22}$$

which represent the integral of square error (ISE), where ψ_d and δ_d represent desired yaw angle and canard demand respectively, and ψ_a and δ_a represent actual yaw angle and canard demand respectively. Additionally, to assess the response speed of the

https://doi.org/10.1017/S0373463300008973 Published online by Cambridge University Press

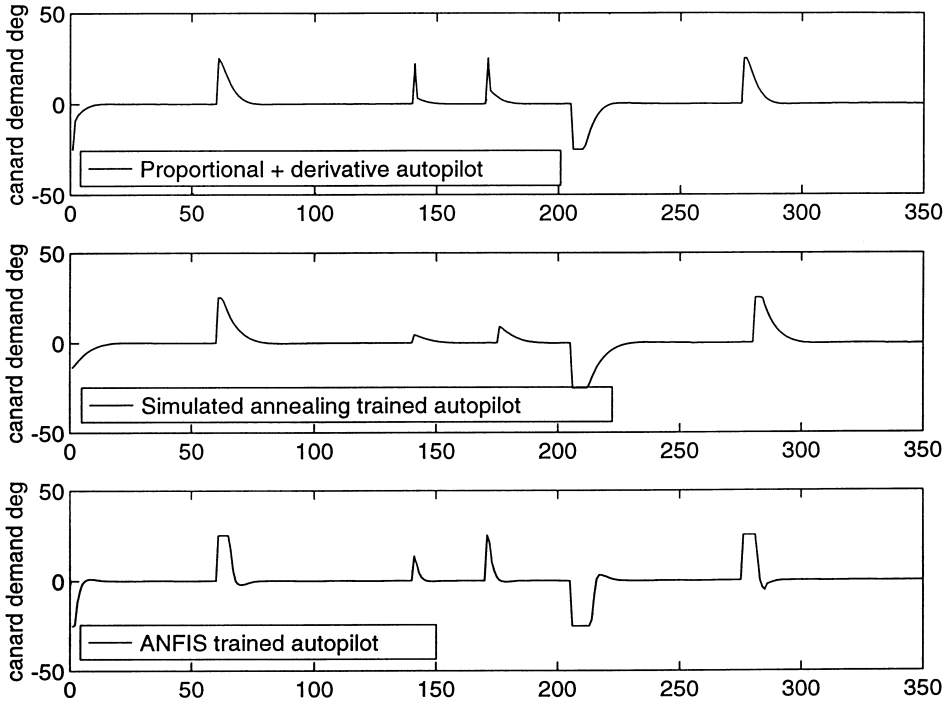

Figure 6. Canard demands of the AUV over the validation track.

Table 2. Yaw responses over a course-changing manoeuvre of 40 degrees.

AUV model	$\psi_e(°)^2$	$\delta_e(°)^2$	T_{RS}	$M_P(t)\%$
		Proportional + Derivative autopilot		
5 knots	124·74	17·28	20·77	1·14
7·5 knots	87·64	11·38	15·16	0·73
10 knots	70·51	8·66	14·90	0·42
		Simulated Annealing autopilot		
5 knots	117·39	18·71	19·98	0·61
7·5 knots	85·46	11·33	15·29	0·01
10 knots	68·58	7·79	14·30	0·01
		ANFIS autopilot		
5 knots	83·18	33·86	9·76	2·86
7·5 knots	59·29	20·98	7·79	1·90
10 knots	46·02	13·90	7·51	1·32

AUV model and the oscillatory nature of each AUV response to a particular autopilot, figures pertaining to the rise time (T_R) and the percentage peak overshoot ($M_P(t)$) were collected. Rise time is considered here as the time to reach 99% of the course-change demand and the percentage peak overshoot is calculated as a relative percentage of the course-change demand.

As parameter tuning took place at 7·5 knots, the robustness of each autopilot was assessed by simulating AUV responses to a course-change of 40° at surge velocities of 5, 7·5 and 10 knots. Table 2 contains the results pertaining to these three surge

https://doi.org/10.1017/S0373463300008973 Published online by Cambridge University Press

velocities. Additionally, data are supplied for off-course error, canard effort, rise time and percentage peak overshoot. When operating at 7·5 knots, the autopilot tuned using the SA technique was 2·49% more accurate than the traditional PD autopilot. This illustrates that the SA-tuned autopilot produces a reduced off-course error for the 40° course-changing demand, as shown in Figure 7. Moreover, the autopilot

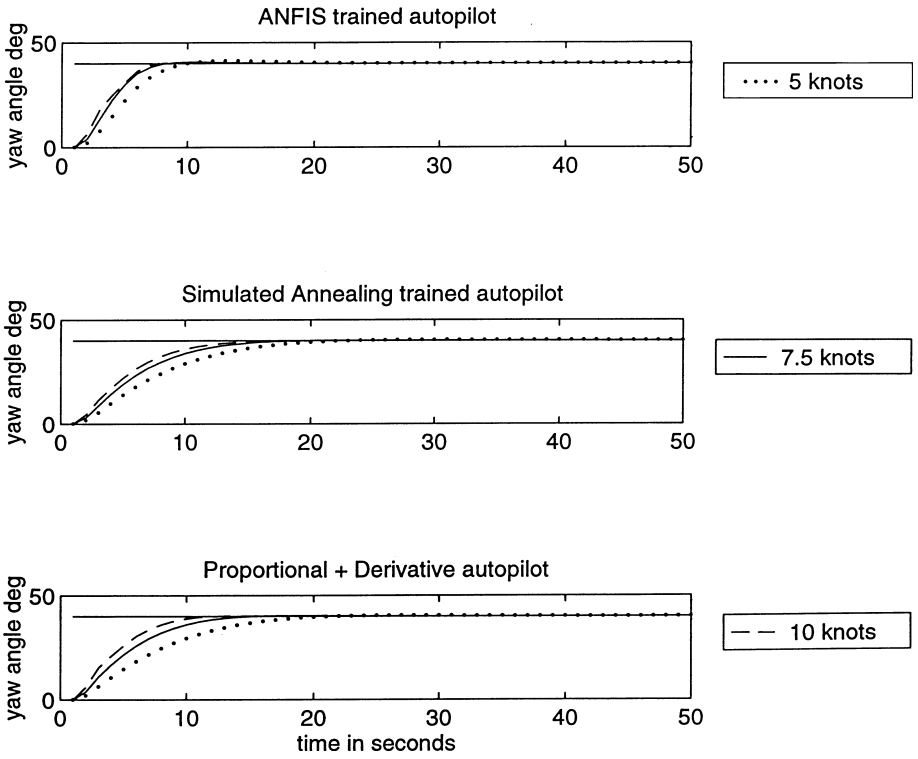

Figure 7. Robustness test of the AUV autopilots.

designed using the ANFIS technique is 32·35% more accurate than the PD autopilot and 30·62% more accurate than the SA-tuned fuzzy autopilot. At 5 knots, the effectiveness of the canard control surfaces is significantly diminished due to the reduced hydrodynamic forces acting on them. Intuitively, one would anticipate more sluggish AUV response times as a consequence of this situation, which is borne out in the results of Table 2. The SA-tuned autopilot again produced course-changing responses that were 5·89% more accurate than the PD autopilot. However, the ANFIS-tuned fuzzy autopilot proved to be 29·14% and 33·32% more accurate than the SA and PD autopilots respectively. Conversely, the increased effectiveness of the canard control surfaces at 10 knots lead to much sharper AUV responses. Figure 7 clearly illustrates the superior performance of the ANFIS-tuned autopilot at 10 knots, with a reduction in off-course error of 32·89% and 34·73% over the SA and PD autopilots respectively.

Use was made of a LOS guidance algorithm (as detailed in Section 7) in order that each autopilot's effectiveness could be examined in the presence of sea current

https://doi.org/10.1017/S0373463300008973 Published online by Cambridge University Press

disturbances. Each autopilot was applied to the course-changing track configuration of Figure 8. To highlight the effect of sea current disturbances, results are presented

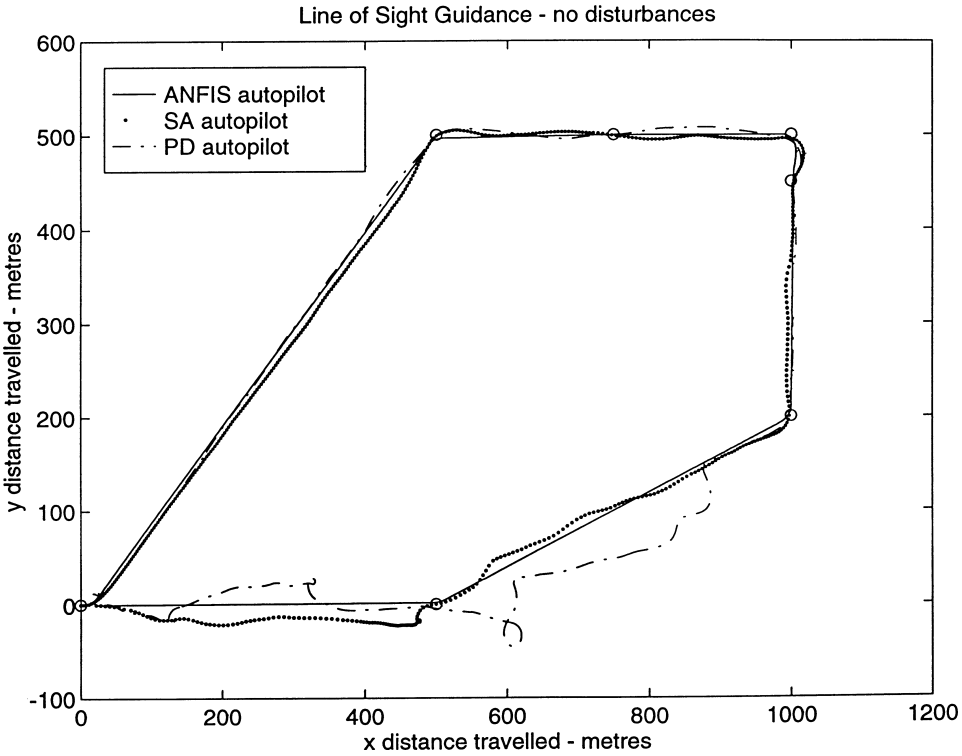

Figure 8. Effectiveness of the line-of-sight guidance systems for waypoint following.

in Figure 8 for no added disturbances and in Figure 9 for a sea current disturbance of one metre per second (in the direction of the positive y-North axis). The circles depicted in Figure 8 represent the target waypoints which are stored within the mission planner prior to mission embarkation. Therefore, the autopilot that traces the shortest distance between these waypoints (whilst visiting all of them) is considered the most effective at the course-changing task.

From Figure 8 it is clearly evident that the ANFIS-tuned fuzzy autopilot is the most effective at following the specified set of target waypoints. The course-following error incurred by employing the ANFIS-tuned autopilot with no current disturbance is considerably less than that of the SA and PD autopilots. Indeed, the inclusion of the current disturbance, as shown in Figure 9, serves to reinforce the superiority of the ANFIS-tuned autopilot, even though the course-following capability of the PD autopilot can be seen to be improved by the addition of the disturbance.

At present there is a great deal of research interest concerning AUV guidance in the NGC community. Typical methods of AUV guidance include dead-reckoning position fixing using speed calculations based upon motor revolutions and torque data taken from the on-board data logger, and also intermittent surfacing of the vehicle to obtain GPS position fixes at pre-specified waypoints.

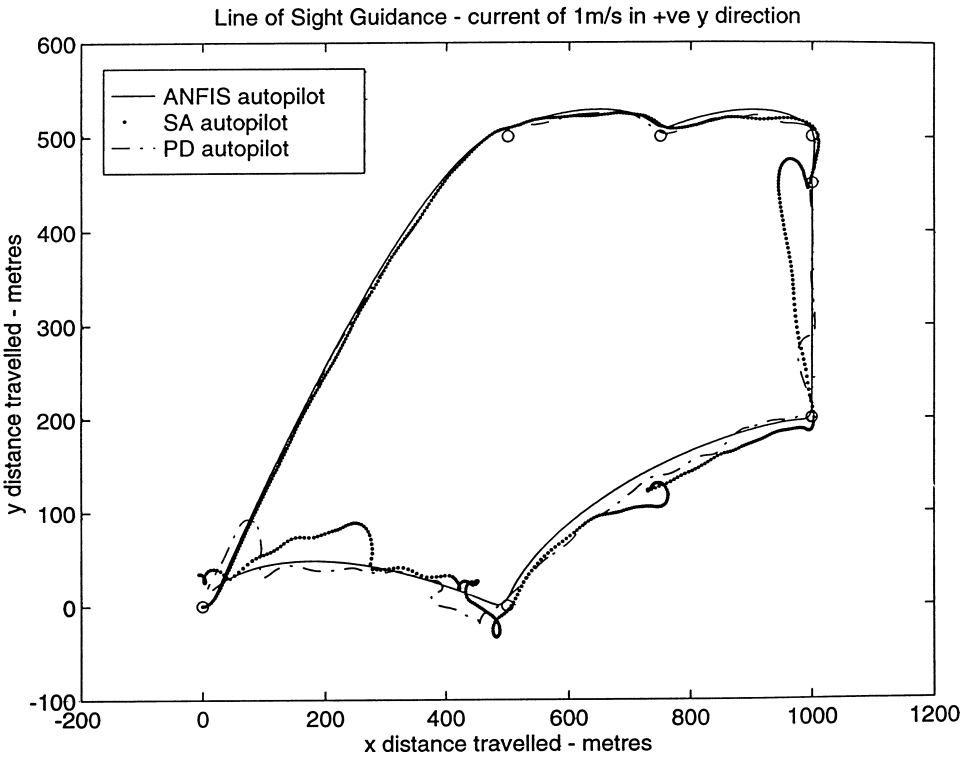

Figure 9. Effectiveness of the line-of-sight guidance systems for waypoint following in the presence of sea current disturbance.

9. CONCLUSIONS. This paper has discussed the tuning of a fuzzy autopilot for course-changing control of an AUV using a neural network architecture and two neural algorithms. The resulting autopilots remain purely fuzzy as parameter tuning is conducted off-line. From the results presented, it may be concluded that the ANFIS approach provides a viable autopilot design solution in the presence of environmental disturbances and changing vehicle surge velocities. The LOS algorithm presented herein is used as a means of effecting AUV guidance. For the purposes of these simulations it is assumed that knowledge of the AUV global coordinates is constantly available underwater.

ACKNOWLEDGEMENTS

The authors wish to thank the DERA, Sea Systems Sector, Winfrith, for supplying the AUV model and their continuing support throughout this work.

REFERENCES

[1] Goodrich, D. (1997). *Marine Foresight Report*, Department of Trade and Industry.
[2] Summerhayes, C. P., Coles, R., Wheeler, B. Baker, M., Cronan, D. S., Burt, R. Griffiths, G., Veck, N., Anderson, D., Young, H. and Murphy, M. (1997). Report of the marine technology foresight panel working group on exploitation of non-living marine resources, *Underwater Technology*, Vol. 22, No. 3, pp. 103–122.

[3] Hawley, J. G. (1993). Diesel engine operation on synthetic atmospheres for underwater applications, *PhD Thesis*, University of Exeter, UK.
[4] Silvestre, C. and Pascoal, A. (1996). Control of an AUV in the vehicle and horizontal planes: system design and tests at sea, *Proceedings of the Third International Symposium on Methods and Models in Automation and Robotics*, Vol. 2, pp. 463–468.
[5] Yoerger, D. R. and Slotine, J. J. E. (1985). Robust trajectory control of underwater vehicles, *IEEE Journal of Oceanic Engineering*, Vol. 10, pp. 462–470.
[6] Katebi, M. R. and Desanj, D. (1996). Integrated predictive control design for autonomous underwater vehicles, *Proceedings of the Thirteenth World Congress of IFAC*, Vol. Q, pp. 327–332, San Francisco, USA.
[7] Jang, J. S. R. (1993). ANFIS: Adaptive Network-Based Fuzzy Inference System, *IEEE Transactions on Systems*, *Man and Cybernetics*, Vol. 23, pp. 665–685.
[8] Craven, P. J. (1999). Intelligent control strategies for an autonomous underwater vehicle, *PhD Thesis*, University of Plymouth.
[9] Kirkpatrick, S., Gelatt C. and Uecchi, M. (1983). Optimisation by simulated annealing, *Science*, Vol. 220, pp. 671–680.
[10] Healey, A. J. and Lienard, D. (1993). Multivariable sliding mode control for autonomous diving and steering of unmanned underwater vehicles, *IEEE Journal of Oceanic Engineering*, Vol. 18, pp. 327–339.